ACS APPLIED MATERIALS & INTERFACES

Research Article

www.acsami.org

Development of Nanocomposite Membranes Containing Modified Si Nanoparticles in PEBAX-2533 as a Block Copolymer and 6FDA-Durene Diamine as a Glassy Polymer

Vajiheh Nafisi and May-Britt Hägg*

Department of Chemical Engineering, Faculty of Natural Science and Technology, Norwegian University of Science and Technology (NTNU), NO-7491 Trondheim, Norway

ABSTRACT: Nanocomposite membranes of modified Si nanoparticles as inorganic filler in two different polymers from two different categories were developed. Synthesized 6FDA-durene diamine as a glassy polymer and PEBAX-2533 as a block copolymer were used as the polymer matrix to develop the nanocomposite membranes of modified Si nanoparticles in polymer matrix. The scanning transmission electron microscopy (STEM) results showed nice nano size dispersion of inorganic nanofillers in the polymer matrix in both cases. Pure gas permeation for the gases CO_2, CH_4, N_2, and O_2 and mixed gas of CO_2−N_2 was carried out at 2 and 6 bar for single gas and 2.6 bar for mixed gas using the developed nanocomposite membranes. The loading of inorganic fillers in the PEBAX-2533 polymer matrix resulted in a dramatic increase in gas permeability for all tested gases, while a decrease was observed for CO_2/N_2 and CO_2/CH_4 selectivities with small amounts of loading of filler. With higher loading of inorganic filler, the selectivity did not change, which is probably due to the formation of nanogap around the nanoparticles in the polymer matrix. The dispersion of the nanoparticle inorganic fillers in 6FDA-durene polymer matrix caused an increase on the fractional free volume of the polymer matrix due to the disruption of the polymer chain in the presence of the inorganic fillers. Hence, this disruption resulted in an increase of gas permeability for both single and mixed gases, also with an increase in CO_2/N_2 and CO_2/CH_4 selectivities.

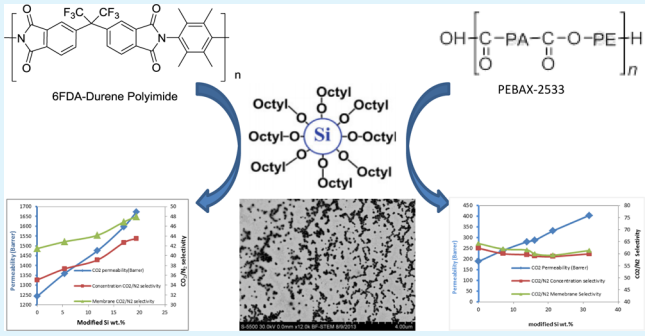

KEYWORDS: *nanocomposite membrane, PEBAX-2533, 6FDA-durene diamine, modified Si nanoparticle, gas separation*

1. INTRODUCTION

Concern about climate change has led to much research and development of new technologies to combat this global challenge. Different options are being considered such as improving energy efficiency, introducing more renewable energy, and enhancing the removal or sequestration rate of CO_2 from the atmosphere, known as CO_2 capture and storage (CCS).[1] A well-known technology for CO_2 capture is based on reversible absorption such as amine scrubbing. This process is energy intensive and poses environmental concerns. Using a membrane gas separation process for CO_2 capture will, however, benefit from advantages such as ease of operation, low-energy consumption, and low environmental impact or footprint.[2]

However, the permeance and selectivity of current commercial polymeric membranes are still too low to be applied for processing large volumes of gas.[3] Polymeric membranes have only the ability to compete with small-scale amine plants operating at less than 30 million standard cubic feet per day.[4] Insufficient thermal and chemical stability and susceptibility to plasticization are other limitations associated with current polymeric membranes. Any improvement in the efficiency of membrane systems could result in considerable financial savings[5] and therefore increase the role of membrane systems in gas separation.

Inorganic membranes are usually made of metals, ceramics, or pyrolyzed carbon.[6] These membranes are increasingly being investigated for gas separation in mixtures of gases due to their well-known chemical and thermal stabilities and much higher gas fluxes or selectivity as compared to those of polymeric membranes. Compared to polymeric membrane, inorganic molecular sieves, such as zeolites and carbon molecular sieves, are excellent materials for gas separation with diffusivity selectivity significantly higher than that of polymeric materials. The accurate size and shape discrimination resulting from the narrow pore distribution ensures superior selectivity.[7]

1.1. Background. Mixed matrix membranes (MMMs) or composite organic−inorganic membranes comprise of inorganic particles dispersed into a continuous polymer matrix. MMMs, in which inorganic fillers (basically nanosized particles) are dispersed in relatively small amounts in a polymer matrix, have been introduced as alternative materials to combine both

Received: January 24, 2014
Accepted: August 26, 2014
Published: August 26, 2014

promising selectivity preference of the inorganic particles and the economical processing potential of polymers.[8]

Permeation of the gases can occur through both the polymeric and inorganic phases. Inorganic particles may function as molecular sieves and disrupt the polymer structure, therefore enhancing the permeance, or they may act as a barrier, decreasing gas permeance.[9] At low to intermediate loading of the inorganic fillers, transport relies upon diffusion through the polymer matrix and across the inorganic particles. Molecular transport occurs primarily across the inorganic phase at very high inorganic loading. However, in some mixed-matrix membranes, selective sorption of different gases occurs by the inorganic phase.[4] At low loadings of the inorganic fillers in organic−inorganic membranes, gas transport primarily occurs through the polymeric matrix. The inorganic materials dispersed into the polymer matrix, including silica particles,[10−12] zeolites,[13−19] carbon nanotubes,[20−22] and metal organic frameworks.[23−25]

One of the inorganic fillers that have received significant attention throughout the development of MMMs is silica nanoparticles that can be categorized into two groups, nonporous silica and ordered mesoporous silica. These fillers are introduced in the polymeric matrix through sol−gel reaction, in which the silica precursors are hydrolyzed and condensed and then dispersed as nanoparticles in the polymer matrix. The dispersion is at the molecular or nano scale level, therefore the interactions between the silica and the organic part can be tailored in order to control the morphological structure at the interface of the phases of inorganic filler and the polymer.[26,27]

The preparation of MMM using impermeable inorganic particles has been dominated by the use of fumed silica as the dispersed phase. Although some grades of fumed silica contain primary particles with diameters on the nano scale, these particles are chemically fused together so that it is impossible to disperse the primary particles individually or as nanoscale aggregates. Because the primary particles are nano scale with respect to their diameter and contain high specific area, these silica particles show improvement in their distribution in the matrix and prevent the formation of nonselective voids in the interface between nanoparticles and polymer. The dispersion of metal oxides normally demonstrates a similar effect as that of impermeable silica particles. The gas transport behavior in such MMMs is influenced by chain packing disruption and agglomeration of nanoparticles on the nano scale in the polymer matrix. Several researchers report using MgO and TiO_2 nanoparticles embedded in mixed matrix membrane.[28−35]

Because the nonporous silica particles are nonpermeable, the dispersion of this inorganic filler into the polymer matrix does not directly contribute to the change of gas separation properties, but it influences the molecular packing of the polymer chains, which results in an improvement of the permeation and the selectivity properties.[36] Particularly, dispersion of nonporous silica in polymer matrix can influence the separation performance in two ways,[37] which can be observed as (1) an increase in polymer free volume without creating nonselective voids, which in turn results in the improvement of gas permeation properties, or (2) the formation of free volume elements large enough to permit nonselective Knudsen transport, resulting in a decrease in selectivity. The void formation in nanoparticles/polymer matrix interface, as well as agglomeration of particles and weak interaction between polymer and nanoparticles at interface, particularly at high loadings, has led to greater permeability compared to that predicted in some reported works.[35] In the present work, silica on the nano scale was used as inorganic fillers in MMMs while it was modified by the organic linkage to have better interaction with the polymer matrix, as shown in Figure 1.[38]

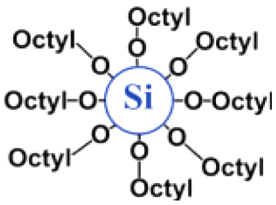

Figure 1. Chemical structure of modified Si nanoparticle.[38]

Polymers, the most widely used materials in membrane gas separation,[39] can be generally categorized on the basis of their glass transition temperature (Tg) as glassy polymers, which operate below their Tg, or rubbery polymers, which operate above their Tg. Glassy polymers are able to effectively discriminate molecules with small differences in molecular dimensions.[40] They are inherently more size- and shape-selective compared to rubbery polymers, and therefore, they can be better candidate for CO_2 separation.[4] In this work, 6FDA-durene diamine was used as one of the polymer matrix to develop mixed matrix membranes due to its proper gas separation properties.

The poly(ether-*b*-amide) Pebax has been known as an appropriate candidate for membrane with the application of separation of H_2 and CO_2. Pebax has received much attention as a CO_2 selective membrane material following its first introduction by researchers in 1990.[41] Pebax is a thermoplastic elastomer that contains a hard aliphatic polyamide (PA) segment, which supplies the mechanical strength, and a soft polyether segment, which provides the gas transport properties.[42,43] Due to the strong affinity of polar ethylene oxide (EO) units to quadrupolar CO_2 molecules, Pebax shows relatively high CO_2 permeability and CO_2/H_2 selectivity.[44]

Recently, much research has been conducted using Pebax or blends of polymers with poly(ethylene oxide) (PEO) to investigate gas permeation properties,[45−49] but less work has been done on MMMs with Pebax as polymer matrix. In the present work, Pebax-2533 as polymer continuous phase was chosen from this category to study permeation of pure CH_4, O_2, N_2, and CO_2 gases. The extent of loading of modified Si on two different cases of mixed matrix membranes was studied, and morphological structure and separation performance of the membranes were evaluated. The developed nanocomposite or mixed matrix membranes are Case 1, mixed matrix membrane of modified Si/6FDA-Duren Diamine, and Case 2, mixed matrix membrane of modified Si/PEBAX-2533.

1.2. Mechanisms of Gas Transport in Nanocomposite Membrane. The gas separation of nanocomposite membranes can be affected in two ways by adding inorganic nanofillers: (1) the interaction between inorganic nanofillers and polymer-chain segments may disrupt or influence the polymer-chain packing, and as a result the voids (free volumes) between the polymer chains increase, hence there will be an increased gas diffusion;[50,51] and (2) some interactions may occur between the hydroxyl and other functional groups on the surface of the inorganic fillers and gases such as CO_2 and SO_2, thereby

increasing the solubility of the penetrant component.[52,53] Different transport mechanisms were introduced in the current work to interpret the gas transport through nanocomposite membranes.[54]

Maxwell's model is often used to model the permeability of composite membranes filled with roughly spherical impermeable particles.[55] The Maxwell's model equation indicates both the loss of membrane solubility due to the loss of polymer volume available for sorption and a decrease in diffusivity due to increment of the penetrant diffusion pathway length.[56] Both factors result in decreasing permeability with increasing particle volume fraction.[57]

The other model is a free volume increase mechanism based on the model introduced by Cohen and Turnbull.[58] According to the model, increments of polymer free volume are expected to enhance penetrant diffusion. The free-volume increase mechanism represents an understanding of the interaction between nanofillers and the segments of polymer-chain. The nanofillers may increase the free volume between the polymer chains due to the disruption of the polymer-chain packing, and as a result, gas diffusion enhances and gas permeability increase.

The solubility increase mechanism is based on the interaction between the nanofillers and penetrants. The solubility of the penetrants in the nanocomposite membranes and, in turn, the gas permeability may increase due to interaction between functional groups, such as hydroxyl, on the surface of the inorganic nanofiller phase with polar gases, such as CO_2 and SO_2;[54] however, this is not fully understood.

Nanogap hypothesis was introduced by Cong et al.[54] for the nanoparticles with better compatibility with the polymer matrix. In their work, trimethylsilyl- or triphenylsilyl-modified silica, was used in brominated poly(2,6-diphenyl-1,4-phenylene oxide) (BPPOdp) to investigate the gas performance of the nanocomposite membranes. The modified nano silica was dispersed more homogeneously in the polymer matrix and resulted in a more efficient disruption of the polymer-chain packing and therefore an increase in the free volume for molecular diffusion and thus gas permeability. Nevertheless, these homogeneous nanocomposite membranes had a substantially lower gas permeability compared to that of the membranes with unmodified silica. Accordingly, they proposed that because of the poor compatibility of the polymer and the silica surface, the polymer chains could not tightly contact the silica nanoparticles; therefore, a narrow gap formed, surrounding the silica particles, as illustrated in Figure 2. The gas diffusivity and permeability were increased due to shortening of the gas diffusion path. This also explained why the addition of the nanoparticles enhanced gas permeability but did not affect the gas selectivity.

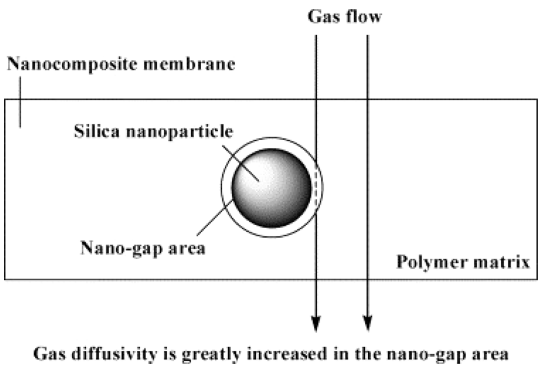

Figure 2. Illustration of nanogap formation in a nanocomposite membrane.[54]

1.3. Theory. For this study, the solution-diffusion mechanism is applied to explain the gas transport properties. The permeability (P) can be expressed as the product of diffusivity (D) and solubility (S).

$$P = DS \tag{1}$$

The ideal selectivity of membranes for pure gases A and B is defined as follows:

$$\alpha_{A,B} = \frac{P_A}{P_B} = \frac{D_A}{D_B}\frac{S_A}{S_B} \tag{2}$$

Where D_A/D_B is diffusivity selectivity and S_A/S_B is solubility selectivity. The permeance in mixed gas was calculated using a complete mixing model from the total permeate flow, as shown in eq 3. The details about the mixed gas permeation setup was well described in previous works in the MEMFO group.[59]

$$Q_A = \frac{J_A}{X_{R,A}P_h - X_{P,A}P_l} \tag{3}$$

where Q_A represents the permeance (m^3(STP)/(m^2 bar h)) of component A (CO_2 or N_2), J_A is the flux (m^3(STP)/m^2h), $X_{R,A}$ and $X_{p,A}$ represent molar concentration (mol %) of the component on feed and permeate side, respectively, and P_h and P_l (bar) are absolute pressure on feed and permeate side, respectively. Two selectivity parameters were reported in this work for mixed gas experiments. Membrane selectivity ($\alpha_{A,B}$) corresponds to the ratio of component A permeance to component B permeance, while concentration selectivity is represented by the ratio of A/B concentration on the permeate side to A/B concentration on the feed side. Concentration selectivity or the separation factor represents a limiting case of the membrane selectivity when the pressure ratio, P_{feed}/P_{perm}, is higher than or equal to selectivity.[60] Concentration selectivity is related to the process conditions[61−63] and is also called process selectivity.

2. EXPERIMENTAL SECTION

2.1. Materials. PEBAX-2533, kindly supplied by Arkema (France), is a block copolymer contain 80 wt % poly(ethylene oxide) (PEO) and 20 wt % polyamide (PA12, nylon-12) and will be further referred to as PEBAX-2533. 6FDA-Durene diamine was synthesized by a two-step poly condensation reaction. More details about the synthesis were explained properly in previous works of the authors.[64] Solvents like chloroform, DMAc, dichloro methylene, and ethanol were purchased from Aldrich. Modified Si nanoparticle was prepared in the Department of Materials Science and Engineering, Norwegian University of Science and Technology, and was received as a solution in ethanol or chloroform.[38]

2.2. Membrane Preparation. PEBAX-2533 was prepared as a flat film membrane by the solvent evaporation method. Ethanol of certified technical grade was used as solvent to make a 3 wt % PEBAX-2533 solution. A calculated amount of PEBAX-2533 was dissolved under reflux condition and stirred at 70 °C for 3−4 h. After the polymer was dissolved completely, the polymer solution was cooled to ambient temperature; a homogeneous solution without gelation was obtained. The dense membrane of pure PEBAX-2533 was obtained by casting 3% polymer solution on a Teflon Petri dish. MMM solutions were prepared by adding proper amounts of modified Si nanoparticle solution to the polymer solution, and the inorganic particles were dispersed in the solution for 20−30 min using ultrasonic mixing. The solution was then poured into a Teflon Petri dish, which was covered with a funnel to avoid any dust in the solution and to allow solvent

evaporation. The casted membrane was dried at room temperature for 1 day and then placed in a vacuum oven at room temperature for 10 h, after which the temperature was gradually increased to 70 °C. The sample was kept at this temperature overnight to completely remove residual solvent. Finally, the temperature was raised to 80 °C and was kept there for 1 h before it was slowly cooled to room temperature. The thickness of achieved membranes varied between 40 and 60 μm. The mixed matrix modified Si nanoparticles/PEBAX-2533 flat sheet membranes were prepared with a membrane area of 5 and 20 cm^2 for single gas and mixed gas permeation tests, respectively.

6FDA-Durene diamine flat sheet dense membranes were also prepared by the solvent evaporation method. Chloroform was used to make a 5 wt % 6FDA-durene diamine solution. After the polymer was completely dissolved in the solvent, the polymer solution was degassed, and the dense membrane of pure 6FDA-durene diamine was obtained by casting the polymer solution on a Teflon Petri dish. To prepare the MMM, a proper amount of modified Si nanoparticle solution in chloroform was added to the polymer solution. The inorganic particles were then ultrasonically dispersed in the polymer solution. The casted membrane was dried at room temperature while it was covered with a closed neck funnel to avoid fast evaporation and prevent dust on the membranes. The dried membranes were placed in a vacuum oven at room temperature for 15 h, and the temperature was gradually increased to 200 °C; it was kept at this temperature overnight to completely remove residual solvent. It was then slowly cooled to room temperature. The thickness of the achieved membranes varied between 40 and 60 μm. The obtained nanocomposite 6FDA-durene diamine/modified Si nanoparticles flat sheet membrane with an area of 5 and 20 cm^2 for single and mixed gas permeation tests, respectively, were used for gas separation characterization.

2.3. Membrane Characterization. *2.3.1. Gas Permeability.* Gas separation performance for MMMs was measured using single gases (N_2, O_2, CH_4, and CO_2) and a binary gas mixture (10% CO_2 and 90% N_2). Single-gas permeation measurements were done with a standard constant volume/variable pressure gas permeation using vacuum on the permeate side. The gas permeance values were calculated from the rate of increase in pressure over time on the permeate side. The single-gas measurements were done at room temperature at 2 and 6 bar. The gas permeability values were obtained by considering the thickness of samples and the measured permeance.

The CO_2 permeability and CO_2/N_2 mixed gas selectivity values of modified Si nanoparticles/(PEBAX-2533 or 6FDA-durene) mixed matrix membranes were determined by measuring the steady state flux of two components in a mixed gas stream permeating through the membrane, where all the process variables such as pressure, relative humidity (RH%) of gases, gas flow rate, temperature, and gas composition were continuously and simultaneously registered by a Lab View program. The temperature and RH% were measured directly inside the feed and sweep gas sides close to the permeation cell. A gas permeation cell with 20 cm^2 membrane active area was used for mixed gas permeation tests.

A mixed gas with composition of 10% CO_2/90% N_2 was used as feed gas, and He was used as a sweep gas. The composition of the permeate gas was analyzed continuously by a 3000 Micro GC gas analyzer (Agilent). The permeance of CO_2 and N_2 was calculated using complete mixing model from the total permeate flow as shown in eq 3. All mixed-gas permeation experiments were performed at 25 °C; relative humidity, 100%; feed pressure, 2.6 bar; and sweep pressure, 1.1 bar, unless otherwise stated.

2.3.2. Wide-Angle X-ray Diffraction (WAXD). In this work, WAXD was used to identify the phase composition of the film, the texture of the film, presence of crystals, and amorphous regions in film. WAXD of pure polymer and MMMs were recorded using Cu Kα radiation of wavelength λ = 1.54060 Å with a graphite monochromator produced by Bruker AXS D8 focus advanced X-ray diffraction meter (Rigaku, Japan, Tokyo) with Ni-filtered. The X-ray scans were taken with a scanning speed of 1°/mm and step size of 0.01°. The angle of diffraction 2θ was varied from 5 to 70° to identify any change in the crystal structure of intermolecular distance between inter segmental chains.

2.3.3. Scanning Electron Microscopy (SEM). In this work, a Hitachi S5500 STEM was used to investigate the cross sections and surfaces of pure membranes and MMMs containing Si inorganic fillers. To avoid charging of samples with electron beam, we covered all samples with a conducting gold coating.

2.3.4. Differential Scanning Calorimetry (DSC). Thermal properties of the pure membranes and MMMs were investigated using a differential scanning calorimeter (TA Q100). A 10 mg sample was put in an aluminum pan covered with a proper lid together with the standard empty pan into the DSC sample holder and heated at the rate of 10 °C/min under N_2 atmosphere.

2.3.5. Thermogravimetric Analysis (TGA). TGA conducted with a thermogravimetric analyzer (Q500, TA Instruments; New Castle, DE) was used to determine the amount or rate of weight changes as a function of temperature over time in controlled atmosphere. About 10 mg of the sample , which was put in the sample holder, was also analyzed by the TGA. He (Helium) was used as purge gas. The heating rate was 10 °C/min.

2.3.6. Density. The density of 6FDA-durene and modified Si nanoparticle/6FDA-durene nanocomposite membrane were measured by using the method of density column containing $ZnCl_2$ solution to calculate the fractional free volume (FFV) of the membranes. The polymer specific volume was then calculated to be 0.4408 cm^3/gr. There is no density data for the PEBAX-2533 membrane and the mixed matrix membranes of this polymer due to practical problems measuring the density of these samples.

3. RESULTS AND DISCUSSION

In this work, modified Si nanoparticles were nicely dispersed in the solvent and polymer matrix. The SEM image in Figure 3 shows the morphology and the size of modified Si nanoparticles. Figures 4 and 5 show by scanning transmission electron microscopy (STEM) the morphology of the nanocomposite membranes of modified Si in PEBAX-2533 polymer matrix. As shown in Figures 4 and 5, the inorganic filler size is around 10−50 nm, and it was well dispersed in polymer matrix. The morphology of nanocomposite membranes of modified Si in 6FDA-duren diamine was investigated by the transmitted electron microscopy of the thin film, as shown in Figure 6. Figure 7 also shows the distribution of nanoparticles in the 6FDA-durene polymer matrix. All of these images were provided by dispersing small amounts of the solutions of mixed matrix on TEM grid to prepare a thin film to be able to have both TEM and SEM images. Due to the size of the inorganic particles, which are almost hidden in the polymer matrix, it was practically impossible to have a clear image of

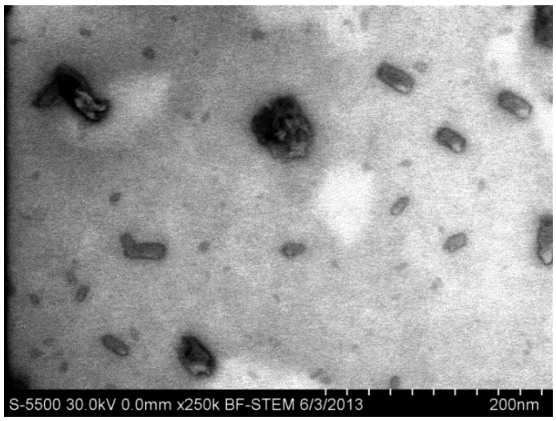

Figure 3. STEM image of modified Si nanoparticle.

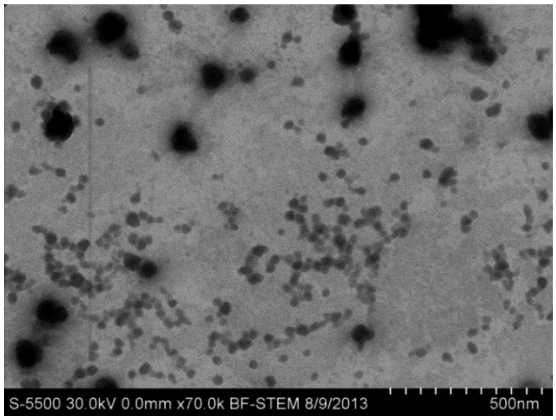

Figure 4. STEM image of modified Si nanoparticle in PEBAX-2533 polymer matrix.

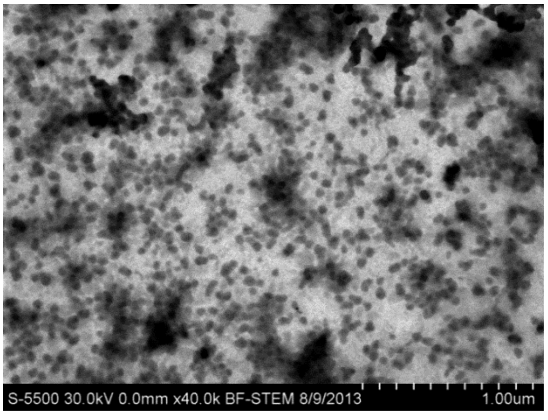

Figure 5. STEM image of modified Si nanoparticle in PEBAX-2533 polymer matrix.

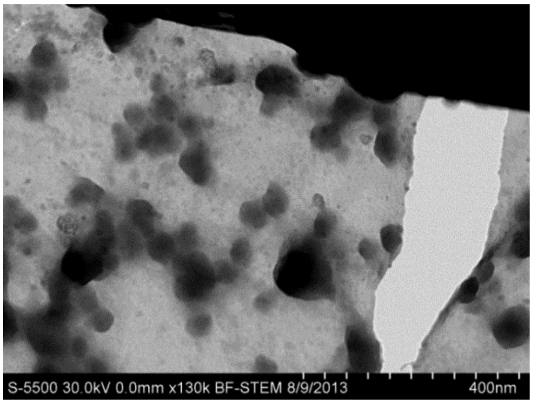

Figure 6. STEM image of modified Si nanoparticle in 6FDA-durene diamine polymer matrix (the white section is not part of the membrane, but shows a broken film).

particles in a cross section of a flat sheet of MMMs. However, the preparation of the thin film on the TEM grid was performed following the method for the preparation of the flat sheet membranes described earlier. The other membrane characterization methods are presented in two separate sections below, and each case discussed separately.

4.1. Case 1: Nanocomposite Membrane of Modified Si-PEBAX-2533. The single-gas separation properties of nanocomposite membranes with different concentration of

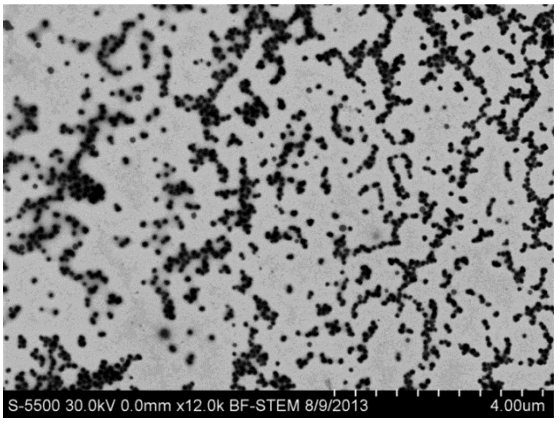

Figure 7. STEM image of modified Si nanoparticle in 6FDA-durene diamine polymer matrix.

modified Si particles were measured. The gas permeability of single gases (CO_2, CH_4, N_2, and O_2 at 2 and 6 bar) and ideal selectivity of the gas pairs CO_2/N_2 and CO_2/CH_4, are shown in Table 1 for different loadings of nanoparticles. The permeability of all gases increases with increasing modified Si nanoparticle concentration. The permeability of CO_2 of pure PEBAX-2533 dense polymeric membrane at 2 bar is 300 Barrer and reaches almost 400 Barrer for the nanocomposite membrane PEBAX-2533/Si-7, while for feed pressure 6 bar, the increment of CO_2 permeability occurs with less slop and changes from 258 Barrer (corresponding to the pure PEBAX-2533) to 298 Barrer for the PEBAX-2533/Si-7. The same trend is observed for N_2 permeability, while for the permeability of CH_4 and O_2, the increase with increasing concentration of modified Si nanoparticles takes place at the same rate for both feed pressures 2 and 6 bar.

The ideal selectivity of CO_2/N_2 drops from 29 for plain polymer to 25, corresponding to PEBAX-2533/Si-4 as the concentration of nanofiller increases, but after that, it remains almost constant and does not change with the addition of more inorganic nanofillers. The observed increment in permeability is due to the increment in free volume as a result of polymer chain interruption. However, the slight decrease in CO_2/N_2 selectivity can be due to the formation of nanogap surrounding the silica particles due to less compatibility with polymer chain segments.

Figure 8 shows the binary CO_2/N_2 mixed gas permeation results as a function of the concentration of modified Si nanoparticles. The permeability of CO_2 in the mixed gas increases dramatically from 189 Barrer for Pure PEBAX-2533 to 404 Barrer with adding 31.7 wt % nanofiller in the polymer matrix. The same trend with respect to ideal gas selectivity was observed for both membrane and concentration selectivity. First, a decrease in CO_2/N_2 selectivity is observed, and then it remains constant or even slightly increases with further increment in the concentration of modifies Si nanoparticles.

The structural changes by the presence of modified silica nanoparticles were characterized with WAXD. The WAXD pattern of modified Si nanoparticle/PEBAX-2533 nanocomposite membrane was compared with those of pure PEBAX-2533 as shown in Figure 9. Generally, the peak from X-ray diffraction of an amorphous polymer is rather broad, while that of a polymer containing a large crystalline region is sharp, and the intensity is strong. A crystalline region of polyamide block via interchain hydrogen bonding results in a strong crystalline peak

Table 1. Summary of Single-Gas Performance of Nanocomposite Membrane of PEBAX-2533/Modified Si with Different Loading of Nanoparticles

		permeability (Barrer)								selectivity at 2 bar	
MMM	modified Si nanoparticle wt %	CO_2 (2 bar)	CO_2 (6 bar)	CH_4 (2 bar)	CH_4 (6 bar)	N_2 (2 bar)	N_2 (6 bar)	O_2 (2 bar)	O_2 (6 bar)	CO_2/N_2	CO_2/CH_4
pure pebax-2533	0	301	259	32	26	10	9	27	21	29.0	9.4
pebax-2533/Si-1	6.5	315	255	35	27	11	9	28	21	28.2	9.0
pebax-2533/Si-2	9.5	318	258	36	29	12	9	29	22	27.1	8.8
pebax-2533/Si-3	12.7	323	260	37	29	12	10	29	22	26.4	8.8
pebax-2533/Si-4	17.2	339	265	38	30	14	10	31	23	25.1	8.9
pebax-2533/Si-5	23.6	363	273	39	33	15	11	35	25	24.5	9.2
pebax-2533/Si-6	26.7	374	282	40	34	15	11	36	27	24.8	9.4
pebax-2533/Si-7	33.3	400	298	43	35	16	11	37	28	24.6	9.4

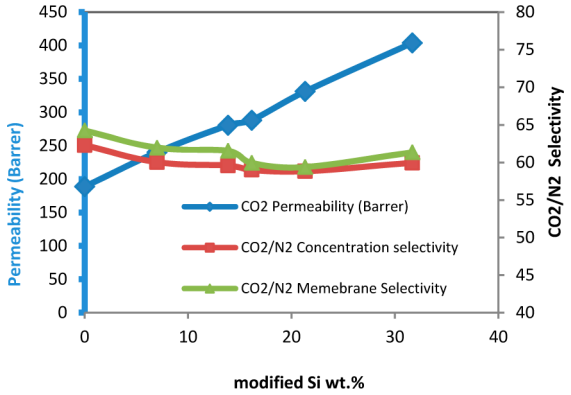

Figure 8. Mixed gas CO_2/N_2 concentration, CO_2 permeability, and membrane selectivity of PEBAX-2533/modified Si nanocomposite membranes as a function of inorganic nanofiller loading.

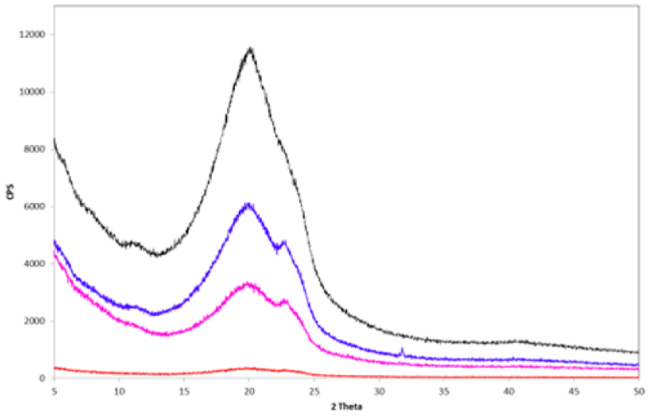

Figure 9. WAXD patterns obtained for (black) PEBAX-2533 polymer membrane and (red, pink, and blue) modified Si nanoparticle/PEBAX-2533 nanocomposite membranes as the concentration of Si particles increases, respectively.

at $2\theta = 20°$ for pure PEBAX-2533.[42,52] The intensity of corresponding peaks in nanocomposite membranes decreases as the modified Si nanoparticle content increases, although there is no shift by the incorporation of silicate. The decrement in the intensity of the corresponding peaks means that the amorphous region in the hybrid has increased. However, a new peak with relatively small intensity is observed in the pattern of hybrid membranes. It is reasonable to suggest that the presence of modified Si nanoparticles considerably disrupts the interchain hydrogen bonding between amide blocks and changes the structure.

The thermal properties of modified Si nanocomposite membranes were investigated and compared to pure PEBAX-2533. As shown in Figure 10, no significant change was

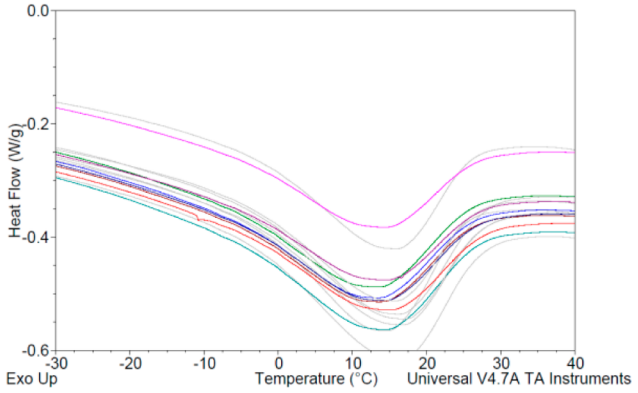

Figure 10. DSC thermograms of the second run of PEBAX-2533 and modified Si/PEBAX-2533 nanocomposites. The gray line is the first run of each sample, and the pink, purple, green, blue, red, and teal lines correspond to pure PEBAX-2533 and MMM of Si-1 to Si-6, respectively.

observed in the melting point of the PE block in the hybrid membranes compared to the pure polymer membrane. This means the disruption that occurred in the polymer chain segment was not strong enough to change the melting point of PE blocks.

The thermal stability and decomposition temperature of pure PEBAX-2533 and nanocomposite membranes with different loadings of modified Si particle were obtained using TGA. As shown in Figure 11, the decomposition temperature of pure PEBAX-2533 membranes starts at 360 °C (blue line), while with increasing content of modified Si nanoparticles in the polymer matrix decomposition starts at higher temperature and changes to 390 °C for the nanocomposite membrane with the highest concentration of inorganic nanofillers.

4.2. Case 2: Nanocomposite Membrane of Modified Si/6FDA-Durene Diamine. The gas permeability of single gases CO_2, CH_4, N_2, and O_2 at 2 and 6 bar and ideal selectivity of gas pairs CO_2/N_2 and CO_2/CH_4 are shown in Table 2 for different loading nanoparticles in 6FDA-durene diamine polymer matrix. The permeability of all gases increases with increasing the modified Si nanoparticle concentration. There is a dramatic increase in CO_2 permeability at 2 bar feed pressure from 1468 to 3785 Barrer, going from pure 6FDA-durene diamine to 6FDA-durene diamine/Si-5 nanocomposite mem-

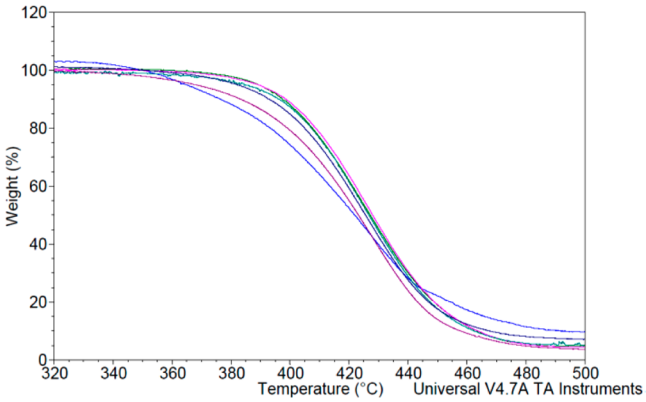

Figure 11. TGA results of PEBAX-2533 and modified Si/PEBAX-2533 nanocomposites membranes. The blue line corresponds to pure PEBAX-2533, while the purple, dark blue, green, and pink lines correspond to MMMs of PEBAX-2533/Si-1 to Si-4, respectively.

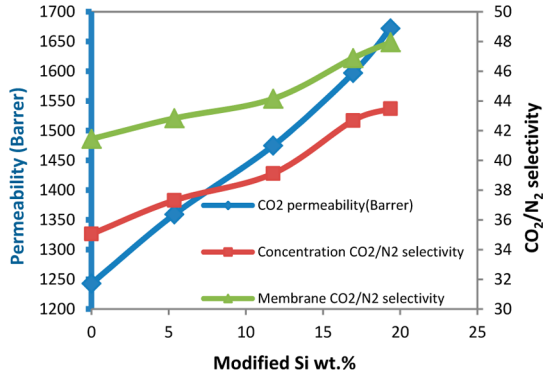

Figure 12. Mixed gas CO_2/N_2 concentration, CO_2 permeability, and membrane selectivity of 6FDA-durene/modified Si nanocomposite membranes as a function of inorganic nanofiller loading.

brane, respectively. The ideal selectivity of CO_2/CH_4 and CO_2/N_2 increases as the loading of modified Si nanoparticles in polymer matrix increases. The CO_2/N_2 ideal selectivity at 2 bar feed pressure increases from 26 for pure 6FDA-durene diamine to 31 for 6FDA-durene diamine/Si-7 nanocomposite membrane, while the CO_2/CH_4 ideal selectivity increases with a higher slope from 23 to 46 for the same samples.

A similar trend was observed for binary mixed gas of CO_2 and N_2, as shown in Figure 12. The permeability of CO_2 increases from 1243 Barrer, corresponding to pure polymer, to 1672 Barrer for nanocomposite membrane with 19.4 wt % nanoparticle loaded in the polymer matrix (Figure 12, blue line). Although it shows a fairly large increase for the permeability of CO_2 in the mixed gas measurements as the loading of nanoparticles increases, the increment of the permeability slope as a function of loadings is less compared to that of single gas; this is as expected for the mixed gas. Both concentration and membrane CO_2/N_2 selectivity increase, as expected and as documented for single-gas measurements.

The increment in permeability and selectivity is due to the increase in free volume confirmed by the density results, as shown in Table 3. The obtained density and fractional free volume (FFV) of nanocomposite membranes with different loadings of nanoparticles are shown in Table 3. As the loading of nanoparticles in 6FDA-durene matrix increases, the density of the flat sheet membrane decreases, and the FFV increases. The density of the MMMs decrease due to interrupted chain packing by the dispersed fillers. This confirms an increased polymer interchain distance that leads to an increased FFV

Table 3. Density and Fraction Free Volume of 6FDA-Durene Flat Sheet Membrane and Mixed Matrix Membrane of Modified Si/6FDA-Durene in Different Nanoparticle Loading in Polymer Matrix

MMM	density g/cm^3	FFV
pure 6FDA-durene	1.3375	0.2335
6FDA-durene/Si-6.3 wt %	1.3137	0.2471
6FDA-durene/Si-8.7 wt %	1.3093	0.2496
6FDA-durene/Si-11.7 wt %	1.2986	0.2557
6FDA-durene/Si-21.0 wt %	1.2661	0.2744
6FDA-durene/Si-30.5 wt %	1.2333	0.2932

which leads to an increment in gas separation performance, as stated earlier in this section.

In addition to SEM imaging, other characterization techniques such as X-ray diffraction were used to confirm the existence of Si nanoparticles in the composite flat sheet membranes, as shown in Figure 13. The backscatter line corresponds to the 6FDA-durene membrane, which has a broad peak in 2θ from 10° to 20°, and shows the amorphous structure of the polymer membrane. Spectra of hybrid dense membranes show the presence of major peaks compared to the spectra of pure polymer, signifying the change in the structure of polymer matrix, as shown in Figure 13, where the red and blue lines correspond to nanocomposite membranes of modified Si nanoparticles.

The thermal stability and decomposition temperature of pure 6FDA-durene and nanocomposite membranes with different loading content of modified Si particle was obtained using a TGA instrument. As shown in Figure 14, the decomposition of pure 6FDA-durene membranes starts above 420 °C (black line), while with the addition of the modified Si nanoparticles

Table 2. Summary of Single Gas Performance of Nanocomposite Membrane of 6FDA-Durene/Modified Si in Different Loading of Nanoparticle

		permeability (Barrer)								selectivity at 2 bar	
MMM	modified Si nanoparticle wt %	CO_2 (2 bar)	CO_2 (6 bar)	CH_4 (2 bar)	CH_4 (6 bar)	N_2 (2 bar)	N_2 (6 bar)	O_2 (2 bar)	O_2 (6 bar)	CO_2/N_2	CO_2/CH_4
pure 6FDA-durene	0	1468	1366	65	68	57	56	207	261	26	23
6FDA-durene/Si-1	6.3	1783	1612	69	70	62	59	219	268	29	26
6FDA-durene/Si-2	8.7	1967	1861	71	72	69	63	228	280	29	28
6FDA-durene/Si-3	11.7	2439	2351	72	73	80	77	260	304	30	34
6FDA-durene/Si-4	21.0	3293	3173	76	75	105	96	329	383	31	43
6FDA-durene/Si-5	30.5	3785	3490	83	81	121	109	347	400	31	46

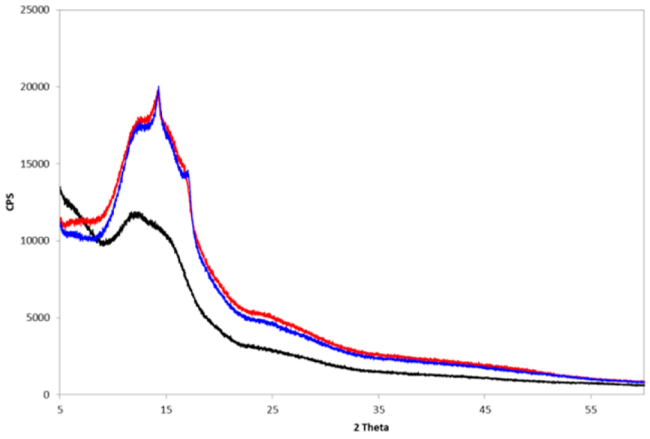

Figure 13. XRD spectra of modified Si/6FDA nanocomposite dense film membranes: (black) 6FDA-durene, (blue) mixed matrix membrane of 6FDA-durene/Si-3, and (red) 6FDA-durene/Si-5 dense film membrane.

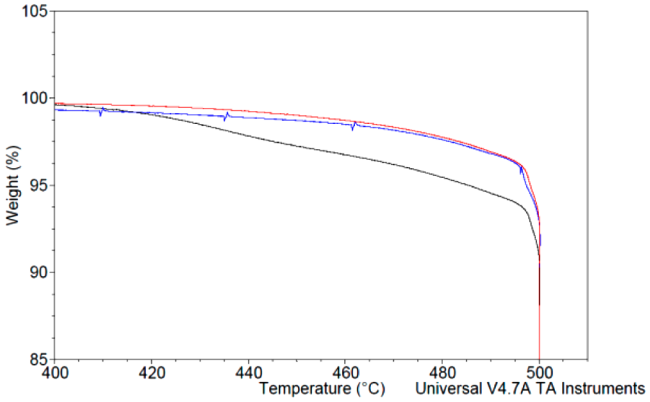

Figure 14. TGA results of (black) 6FDA-durene and modified (blue) Si/6FDA-durene/Si-2 and (red) Si-4 nanocomposites membranes.

into the polymer matrix, decomposition starts at a higher temperature and changes up to 495 °C for the nanocomposite membrane (blue and red lines), corresponding to 6FDA-durene/Si-2 and 6FDA-durene/Si-4 nanocomposite membranes, respectively.

The thermal properties of modified Si nanocomposite membranes were investigated and compared to those of pure 6FDA-durene. Figure 15 shows the second run of the DSC

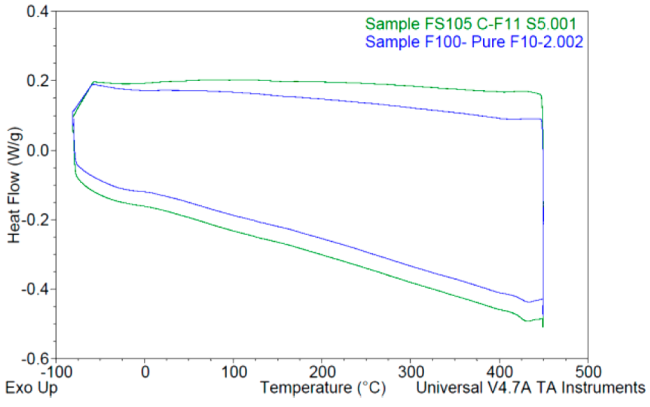

Figure 15. DSC thermograms of the second run of (blue) 6FDA-durene and (green) 6FDA-durene/Si-4 nanocomposite membranes.

thermograms of pure 6FDA-durene membrane (blue line) and modified Si nanocomposite membrane in 6FDA-durene polymer matrix (green line). No significant change was observed in the Tg of the 6FDA-durene/modified Si hybrid membranes compared to that of the pure polymer membrane.

CONCLUSIONS

The organic–inorganic hybrid membranes of modified Si nanoparticles in two different polymer matrixes, PEBAX-2533 and 6FDA-durene diamine, respectively, were successfully prepared and characterized. The hybrid membranes exhibited much higher gas permeability for both single-gas and mixed-gas permeation tests compared to that of the pure polymers in both cases. In the PEBAX-2533/modified Si nanoparticle composite membrane, the increase in permeability was not as dramatic as that of the synthesized 6FDA-durene diamine with nanoparticles. This is because the PEBAX is a block copolymer containing both soft and hard segments, while 6FDA-durene is a glassy polymer, and the disruption of the chains by adding nanoparticles creates a significantly larger FFV (~18% for 21 wt % added nanoparticles). For PEBAX-2533, there was a small drop in selectivity with the addition of nanofillers, after which the selectivity remained constant. This may be due to the formation of nanogaps in contact between nanoparticles and polymer chain segments; it may also be due to how the nanoparticles are distributed within this block copolymer containing both hard and soft segments. The disruption of polymer chain segments caused by the presence of modified Si nanoparticles in both polymers resulted in high permeability of these hybrid membranes. This disruption was confirmed by XRD results; however, it is not strong enough to be visible as a change in melting point of PE blocks.

The CO_2/N_2 and CO_2/CH_4 ideal selectivity of 6FDA-durene also increased significantly with the loading of inorganic nanofiller. This increase in both permeability and selectivity is clearly a result of the polymer chain disruption, which is also confirmed by the density results showing an increase in the FFV of the matrix. The change in the morphology was confirmed by XRD results. However, the Tg of the polymer matrix did not change with the presence of the inorganic filler, but a change in decomposition temperature was observed.

AUTHOR INFORMATION

Corresponding Author

*E-mail: may-britt.hagg@chemeng.ntnu.no.

Notes

The authors declare no competing financial interest.

ACKNOWLEDGMENTS

This work was financially supported by a BIGCCS project as a part of the PhD work of the first author. The authors would like to thank Dr. Alberto Ruíz Treviño and his student, Suzanne Sánchez García, for doing the density measurement in their lab and Mustafa Balci for preparing the modified Si nanoparticle solutions.

REFERENCES

(1) Favre, E. Carbon Dioxide Recovery From Post-Combustion Processes: Can Gas Permeation Membranes Compete with Aabsorption? *J. Membr. Sci.* **2007**, *294* (1–2), 50–59.

(2) Sridhar, S.; Smitha, B.; Aminabhavi, T. M. Separation of Carbon Dioxide from Natural Gas Mixtures through Polymeric Membranes—A Review. *Sep. Purif. Rev.* **2007**, *36* (2), 113–174.

(3) Iarikov, D. D.; Oyama, S. T. Review of CO_2/CH_4 Separation Membranes. In *Membrane Science and Technology*, Oyama, S. T.; Stagg-Williams, S., Eds. Elsevier: 2011; pp 91−115.
(4) Baker, R. W. *Membrane Technology and Applications*. John Wiley & Sons, Ltd., England, 2004.
(5) Visser, T.; Masetto, N.; Wessling, M. Materials Dependence of Mixed Gas Plasticization Behavior in Asymmetric Membranes. *J. Membr. Sci.* **2007**, *306* (1−2), 16−28.
(6) Morooka, S.; Kusakabe, K. Microporous Inorganic Membranes for Gas Separation. *MRS Bull.* **1999**, *24* (03), 25−29.
(7) Koresh, J.; Soffer, A. Study of Molecular Sieve Carbons. Part 2.—Estimation of Cross-Sectional Diameters of Non-Spherical Molecules. *J. Chem. Soc., Faraday Trans. 1* **1980**, *76* (0), 2472−2485.
(8) Shekhawat, D.; Luebke, D. R.; Pennline, H.W. A Review of Carbon Dioxide Selective Membranes: A Topical Report; DOE/NETL-2003/1200; U.S. Department of Energy: Washington, DC, 2003.
(9) Scholes, C. A.; Kentish, S. E.; Stevens, G. W. Carbon Dioxide Separation Through Polymeric Membrane Systems for Flue Gas Applications. *Recent Pat. Chem. Eng.* **2008**, *1* (1), 52−66.
(10) Suzuki, T.; Yamada, Y. Characterization of 6FDA-Based Hyperbranched and Linear Polyimide−Silica Hybrid Membranes by Gas Permeation and 129Xe NMR Measurements. *J. Polym. Sci., Part B: Polym. Phys.* **2006**, *44* (2), 291−298.
(11) Juhyeon, A.; Chung, W.-J.; Pinnau, I.; Song, J.; Du, N.; Robertson, G. P.; Guiver, M. D. Gas Transport Behavior of Mixed-Matrix Membranes Composed of Silica Nanoparticles in a Polymer of Intrinsic Microporosity (PIM-1). *J. Membr. Sci.* **2010**, *346*, 280−287.
(12) Ahn, J.; Chung, W.-J.; Pinnau, I.; Guiver, M. D. Polysulfone/Silica Nanoparticle Mixed-Matrix Membranes for Gas Separation. *J. Membr. Sci.* **2008**, *314* (1−2), 123−133.
(13) Li, Y.; Chung, T. S.; Kulprathipanja, S. Novel Ag^+−Zeolite/Polymer Mixed Matrix Membranes with a High CO_2/CH_4 Selectivity. *AIChE J.* **2007**, *53* (3), 610−616.
(14) Husain, S.; Koros, W. J. Mixed Matrix Hollow Fiber Membranes Made with Modified HSSZ-13 Zeolite in Polyetherimide Polymer Matrix for Gas Separation. *J. Membr. Sci.* **2007**, *288* (1−2), 195−207.
(15) Şen, D.; Kalıpçılar, H.; Yilmaz, L. Development of Polycarbonate Based Zeolite 4A Filled Mixed Matrix Gas Separation Membranes. *J. Membr. Sci.* **2007**, *303* (1−2), 194−203.
(16) Süer, M. G.; Baç, N.; Yilmaz, L. Gas Permeation Characteristics of Polymer−Zeolite Mixed Matrix Membranes. *J. Membr. Sci.* **1994**, *91* (1−2), 77−86.
(17) Ismail, A. F.; Kusworo, T. D.; Mustafa, A. Enhanced Gas Permeation Performance of Polyethersulfone Mixed Matrix Hollow Fiber Membranes Using Novel Dynasylan Ameo Silane Agent. *J. Membr. Sci.* **2008**, *319* (1−2), 306−312.
(18) Hillock, A. M. W.; Miller, S. J.; Koros, W. J. Crosslinked Mixed Matrix Membranes for the Purification of Natural Gas: Effects of Sieve Surface Modification. *J. Membr. Sci.* **2008**, *314* (1−2), 193−199.
(19) Li, Y.; Chung, T. S. Highly Selective Sulfonated Polyethersulfone (SPES)-Based Membranes with Transition Metal Counterions for Hydrogen Recovery and Natural Gas Separation. *J. Membr. Sci.* **2008**, *308* (1−2), 128−135.
(20) Kim, S.; Chen, L.; Johnson, J. K.; Marand, E. Polysulfone and Functionalized Carbon Nanotube Mixed Matrix Membranes for Gas Separation: Theory and Experiment. *J. Membr. Sci.* **2007**, *294* (1−2), 147−158.
(21) Murali, R. S.; Sridhar, S.; Sankarshana, T.; Ravikumar, Y. V. L Gas Permeation Behavior of Pebax-1657 Nanocomposite Membrane Incorporated with Multiwalled Carbon Nanotubes. *Ind. Eng. Chem. Res.* **2010**, *49* (14), 6530−6538.
(22) Ge, L.; Zhu, Z.; Li, F.; Liu, S.; Wang, L.; Tang, X.; Rudolph, V. Investigation of Gas Permeability in Carbon Nanotube (CNT)−Polymer Matrix Membranes via Modifying CNTs with Functional Groups/Metals and Controlling Modification Location. *J. Phys. Chem. C* **2011**, *115* (14), 6661−6670.
(23) Zhang, Y.; Musselman, I. H.; Ferraris, J. P.; Balkus, K. J., Jr. Gas Permeability Properties of Matrimid® Membranes Containing the Metal−Organic Framework Cu-BPY-HFS. *J. Membr. Sci.* **2008**, *313* (1−2), 170−181.
(24) Ordoñez, M. J. C.; Balkus, K. J., Jr.; Ferraris, J. P.; Musselman, I. H. Molecular Sieving Realized with ZIF-8/Matrimid® Mixed-Matrix Membranes. *J. Membr. Sci.* **2010**, *361* (1−2), 28−37.
(25) Perez, E. V.; Balkus, K. J., Jr.; Ferraris, J. P.; Musselman, I. H. Mixed-Matrix Membranes Containing MOF-5 for Gas Separations. *J. Membr. Sci.* **2009**, *328* (1−2), 165−173.
(26) Joly, C.; Smaihi, M.; Porcar, L.; Noble, R. D. Polyimide−Silica Composite Materials: How Does Silica Influence Their Microstructure and Gas Permeation Properties? *Chem. Mater.* **1999**, *11* (9), 2331−2338.
(27) Morteza, S.; Semsarzadeh, M. A.; Moadel, H. Enhancement of the Gas Separation Properties of Polybenzimidazole (PBI) Membrane by Incorporation of Silica Nano Particles. *J. Membr. Sci.* **2009**, *331*, 21−30.
(28) Hosseini, S. S.; Li, Y.; Chung, T.-S.; Liu, Y. Enhanced Gas Separation Performance of Nanocomposite Membranes Using MgO Nanoparticles. *J. Membr. Sci.* **2007**, *302*, 207−217.
(29) Matteucci, S.; Kusuma, V. A.; Kelman, S. D.; Freeman, B. D. Gas Transport Properties of MgO Filled Poly(1-trimethylsilyl-1-propyne) Nanocomposites. *Polymer* **2008**, *49* (6), 1659−1675.
(30) Matteucci, S.; Raharjo, R. D.; Kusuma, V. A.; Swinnea, S.; Freeman, B. D. Gas Permeability, Solubility, and Diffusion Coefficients in 1,2-Polybutadiene Containing Magnesium Oxide. *Macromolecules* **2008**, *41* (6), 2144−2156.
(31) Matteucci, S.; Kusuma, V. A.; Swinnea, S.; Freeman, B. D. Gas Permeability, Solubility and Diffusivity in 1,2-Polybutadiene Containing Brookite Nanoparticles. *Polymer* **2008**, *49* (3), 757−773.
(32) Matteucci, S.; Kusuma, V. A.; Sanders, D.; Swinnea, S.; Freeman, B. D. Gas Transport in TiO_2 Nanoparticle-Filled Poly(1-trimethylsilyl-1-propyne). *J. Membr. Sci.* **2008**, *307* (2), 196−217.
(33) Shao, L.; Samseth, J.; Hägg, M.-B. Crosslinking and Stabilization of Nanoparticle Filled PMP Nanocomposite Membranes for Gas Separations. *J. Membr. Sci.* **2009**, *326* (2), 285−292.
(34) Shao, L.; Samseth, J.; Hägg, M.-B. Crosslinking and Stabilization of Nanoparticle Filled Poly(1-trimethylsilyl-1-propyne) Nanocomposite Membranes for Gas Separations. *J. Appl. Polym. Sci.* **2009**, *113* (5), 3078−3088.
(35) Moghadam, F.; Vasheghani-Farahani, E.; Omidkhah, M. R.; Pedram, M. Z.; Dorosti, F. The Effect of TiO_2 Nanoparticles on Gas Transport Properties of Matrimid 5218-Based Mixed Matrix Membranes. *Sep. Purif. Technol.* **2011**, 128−136.
(36) Ferrari, M. C.; Galizia, M.; De Angelis, M. G.; Sarti, G. C. Gas and Vapor Transport in Mixed Matrix Membranes Based on Amorphous Teflon AF1600 and AF2400 and Fumed Silica. *Ind. Eng. Chem. Res.* **2010**, *49* (23), 11920−11935.
(37) Gomes, D.; Nunes, S. P.; Peinemann, K.-V. Membranes for Gas Separation Based on Poly(1-trimethylsilyl-1-propyne)−Silica Nanocomposites. *J. Membr. Sci.* **2005**, *246*, 13−25.
(38) Balci, M.; Maria, J.; Vullum-Bruer, F.; Lindgren, M.; Grande, T.; Einarsrud, M.-A. Synthesis of Monodisperse Silicon Quantum Dots Through a K-Naphthalide Reduction Route. *J. Cluster Sci.* **2012**, *23* (2), 421−435.
(39) Abetz, V.; Brinkmann, T.; Dijkstra, M.; Ebert, K.; Fritsch, D.; Ohlrogge, K.; Paul, D.; Peinemann, K. V.; Pereira-Nunes, S.; Scharnagl, N. Developments in Membrane Research: From Material via Process Design to Industrial Application. *Adv. Eng. Mater.* **2006**, *8* (5), 328−358.
(40) Zolandz, R. R.; Fleming, G. K., Theory., In *Membrane Handbook*; Ho, W. S. W., Sirkar, K. K., Eds.; Van Nostrand Reinhold: New York, 1992; pp 25−53.
(41) Blume, I.; Pinnau, I. Composite Membrane, Method of Preparation and Use. US4963165 A, 1990.
(42) Bondar, V. I.; Freeman, B. D.; Pinnau, I. Gas Transport Properties of Poly(ether-*b*-amide) Segmented Block Copolymers. *J. Polym. Sci., Part B: Polym. Phys.* **2000**, *38* (15), 2051−2062.

(43) Bondar, V. I.; Freeman, B. D.; Pinnau, I. Gas sorption and Characterization of Poly(ether-*b*-amide) Segmented Block Copolymers. *J. Polym. Sci., Part B: Polym. Phys.* **1999**, *37* (17), 2463−2475.
(44) Kim, J. H.; Ha, S. Y.; Lee, Y. M. Gas Permeation of Poly(amide-6-*b*-ethylene oxide) Copolymer. *J. Membr. Sci.* **2001**, *190* (2), 179−193.
(45) Yave, W.; Car, A.; Funari, S. S.; Nunes, S. P.; Peinemann, K.-V. CO_2-Philic Polymer Membrane with Extremely High Separation Performance. *Macromolecules* **2009**, *43* (1), 326−333.
(46) Yave, W.; Car, A.; Peinemann, K.-V.; Shaikh, M. Q.; Rätzke, K.; Faupel, F. Gas Permeability and Free Volume in Poly(amide-*b*-ethylene oxide)/polyethylene Glycol Blend Membranes. *J. Membr. Sci.* **2009**, *339* (1−2), 177−183.
(47) Car, A.; Stropnik, C.; Yave, W.; Peinemann, K.-V. PEG Modified Poly(amide-*b*-ethylene oxide) Membranes for CO_2 Separation. *J. Membr. Sci.* **2008**, *307* (1), 88−95.
(48) Car, A.; Stropnik, C.; Yave, W.; Peinemann, K.-V. Tailor-Made Polymeric Membranes Based on Segmented Block Copolymers for CO_2 Separation. *Adv. Funct. Mater.* **2008**, *18* (18), 2815−2823.
(49) Buonomenna, M.; Yave, W.; Golemme, G. Some Approaches for High Performance Polymer Based Membranes for Gas Separation: Block Copolymers, Carbon Molecular Sieves, and Mixed Matrix Membranes. *RSC Adv.* **2012**, *2* (29), 10745−10773.
(50) Merkel, T. C.; Freeman, B. D.; He, Z.; Pinnau, I.; Meakin, P.; Hill, A. J. Ultrapermeable, Reverse-Selective Nanocomposite Membranes. *Science* **2002**, *296*, 519−522.
(51) Moaddeb, M.; Koros, W. J. Gas Transport Properties of Thin Polymeric Membranes in the Presence of Silicon Dioxide Particles. *J. Membr. Sci.* **1997**, *125* (1), 143−163.
(52) Kim, J. H.; Lee, Y. M. Gas Permeation Properties of Poly(amide-6-*b*-ethylene oxide)−Silica Hybrid Membranes. *J. Membr. Sci.* **2001**, *193* (2), 209−225.
(53) Hu, Q.; Marand, E.; Dhingra, S.; Fritsch, D.; Wen, J.; Wilkes, G. Poly(amide-imide)/TiO_2 Nano-Composite Gas Separation Membranes: Fabrication and Characterization. *J. Membr. Sci.* **1997**, *135*, 65−79.
(54) Cong, H.; Radosz, M.; Towler, B. F.; Shen, Y. Polymer−Inorganic Nanocomposite Membranes for Gas Separation. *Sep. Purif. Technol.* **2007**, *55* (3), 281−291.
(55) Barrer, R. M.; Barrie, J. A.; Rogers, M. G. Heterogeneous Membranes: Diffusion in Filled Rubber. *J. Polym. Sci., Part A: Gen. Pap.* **1963**, *1* (8), 2565−2586.
(56) Merkel, T. C.; Freeman, B. D.; Spontak, R. J.; He, Z.; Pinnau, I.; Meakin, P.; Hill, A. J. Sorption, Transport, and Structural Evidence for Enhanced Free Volume in Poly(4-methyl-2-pentyne)/ Fumed Silica Nanocomposite Membranes. *Chem. Mater.* **2003**, *15*, 109−123.
(57) Freeman, B. D. Novel Nanocomposite Membrane Structure for H_2 Separation; University of Texas at Austin: Austin, TX, 2005.
(58) Cohen, M. H.; Turnbull, D. Molecular Transport in Liquids and Glasses. *J. Chem. Phys.* **1959**, *31* (5), 1164−1169.
(59) Sandru, M. Development of a FSC Membrane for Selective CO_2 Capture. Ph.D. Dissertation, Norwegian University of Science and Technology, 2009.
(60) Baker, R. W. *Membrane Technology and Applications*. Wiley: Chicester, 2012.
(61) Zhao, L.; Riensche, E.; Menzer, R.; Blum, L.; Stolten, D. A Parametric Study of CO_2/N_2 Gas Separation Membrane Processes for Post-Combustion Capture. *J. Membr. Sci.* **2008**, *325* (1), 284−294.
(62) Pfromm, P. H.; Pinnau, I.; Koros, W. J. Gas Transport Through Integral-Asymmetric Membranes: A Comparison to Isotropic Film Transport Properties. *J. Appl. Polym. Sci.* **1993**, *48* (12), 2161−2171.
(63) Wijmans, J. G.; Baker, R. W. A Simple Predictive Treatment of the Permeation Process in Pervaporation. *J. Membr. Sci.* **1993**, *79* (1), 101−113.
(64) Nafisi, V.; Hägg, M.-B. Gas Separation Properties of ZIF-8/6FDA-Durene Diamine Mixed Matrix Membrane. *Sep. Purif. Technol.* **2014**, *128* (2014), 31−38.